
2º Capstone Project
Human Activity Recognition
Using Smartphones
Train
& Test
Features
Dataset
galvanize
Nei Rosa da Costa
April - 2018


2º Capstone Project
Human Activity Recognition
Using Smartphones
Train
& Test
Features
Dataset
galvanize
Nei Rosa da Costa
April - 2018

Data set

Abstract:

Human Activity Recognition database built from the recordings of 30 subjects performing activities of daily living (ADL) while carrying a waist-mounted smartphone with embedded inertial sensors.

Source:

(http://archive.ics.uci.edu/ml/datasets/Human+Activity+Recognition+Using+Smartphones)

How the data were collected?

The experiments have been carried out with a group of 30 volunteers within an age bracket of 19-48 years. Each person performed six activities (WALKING, WALKING UPSTAIRS, WALKING DOWNSTAIRS, SITTING, STANDING, LAYING) wearing a smartphone (Samsung Galaxy S II) on the waist. Using its embedded accelerometer and gyroscope, we captured 3-axial linear acceleration and 3-axial angular velocity at a constant rate of 50Hz.

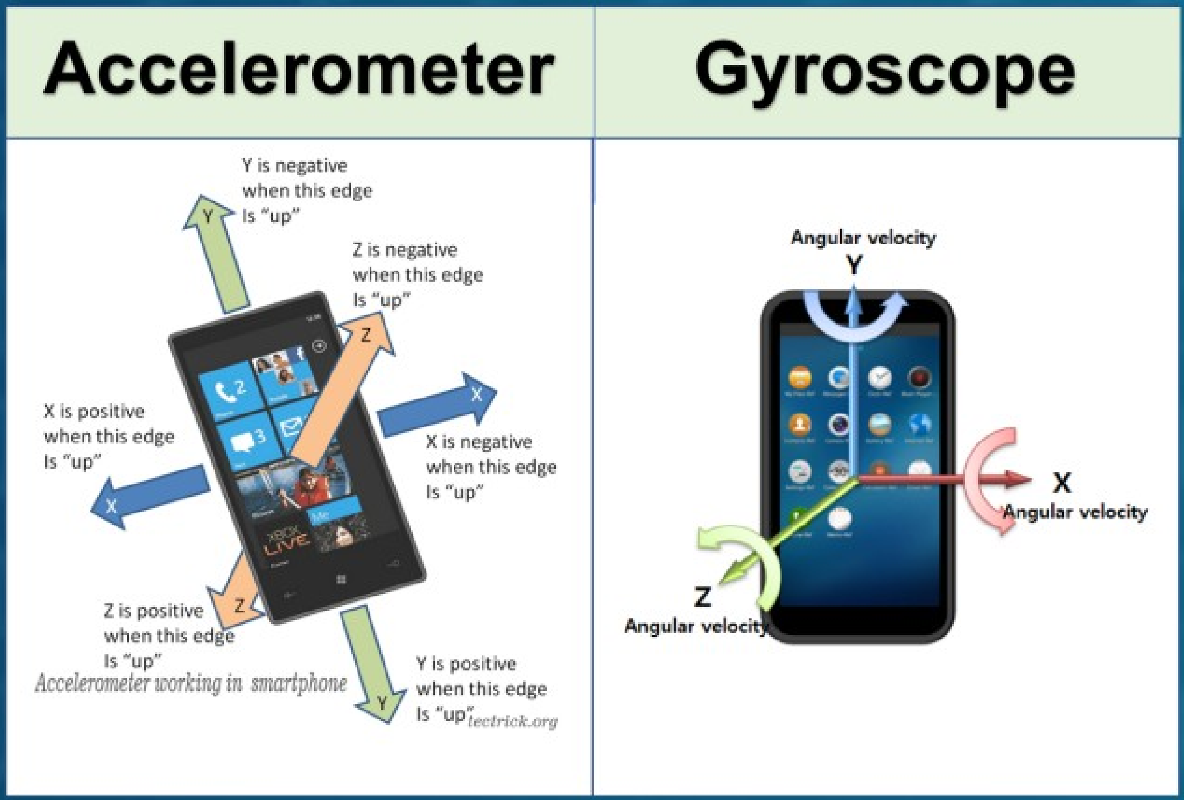

The sensor signals (accelerometer and gyroscope) were pre-processed by applying noise filters and then sampled in fixed-width sliding windows of 2.56 sec and 50% overlap (128 readings/ window)


2º Capstone Project
Human Activity Recognition
Using Smartphones
Train
& Test
Features
Dataset
galvanize
Nei Rosa da Costa
April - 2018

Who was responsible for collecting the data?

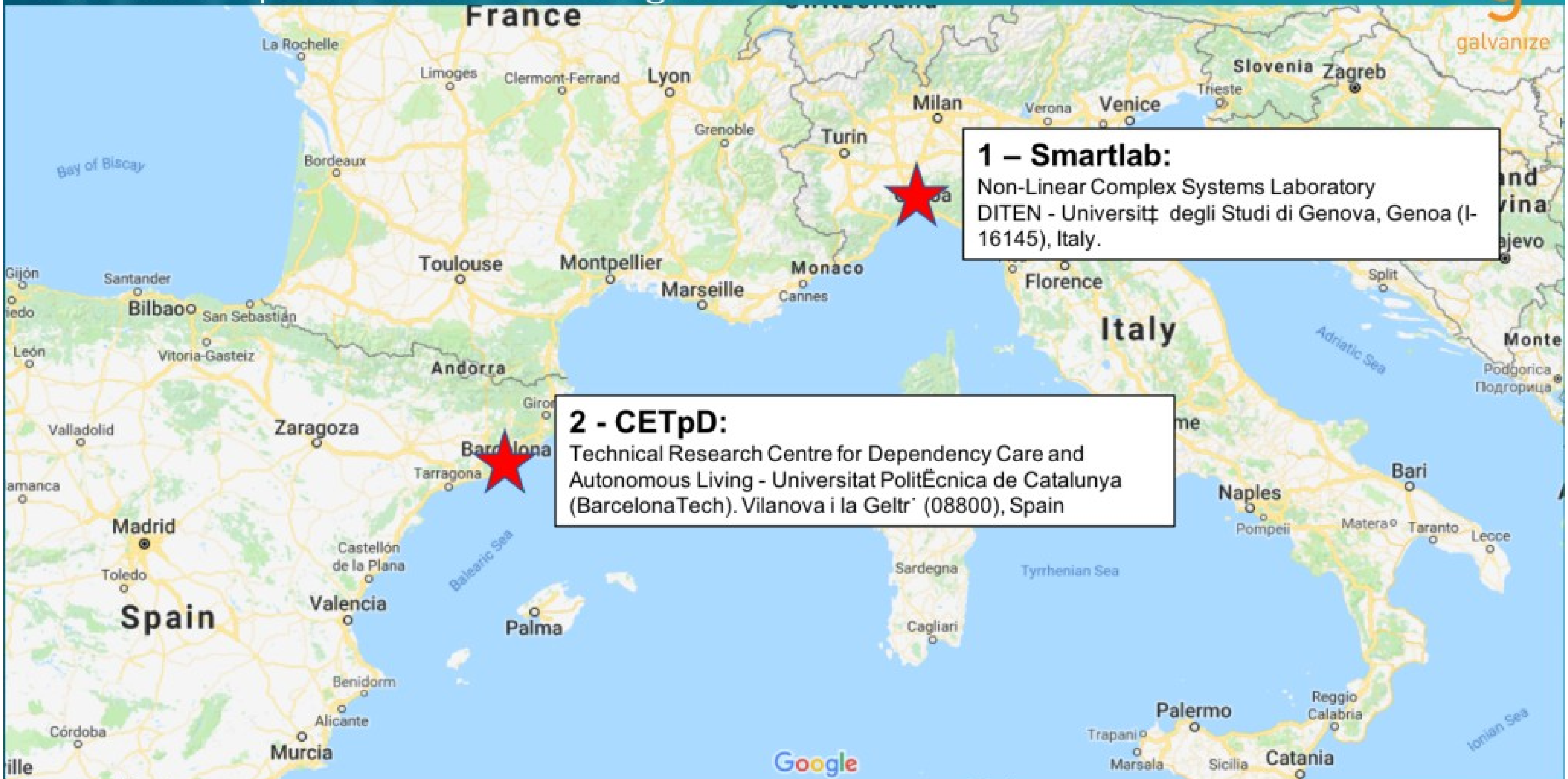


2º Capstone Project
Human Activity Recognition
Using Smartphones
Train
& Test
Features
Dataset
galvanize
Nei Rosa da Costa
April - 2018

Train	Test	Total
21	9	30
7,352 71.39%	2,947 28.61%	10,299

Activity	Train	Test	Total
0 - WALKING	1,226	496	1,722 16.72%
1 - WALKING UPSTAIRS	1,073	471	1,544 14.99%
2 - WALKING DOWNSTAIRS	986	420	1,406 13.65%
3 - SITTING	1,286	491	1,777 17.25%
4 - STANDING	1,374	532	1,906 18.51%
5 - LAYING	1,407	537	1,944 18.88%

galvanize


2º Capstone Project
Human Activity Recognition
Using Smartphones
Train
& Test
Features
Dataset
galvanize
Nei Rosa da Costa
April - 2018

The features selected for this database come from the accelerometer and gyroscope 3-axial raw signals tAcc-XYZ and tGyro-XYZ. These time domain signals (prefix 't' to denote time) were captured at a constant rate of 50 Hz. Then they were filtered using a median filter and a 3rd order low pass Butterworth filter with a corner frequency of 20 Hz to remove noise. Similarly, the acceleration signal was then separated into body and gravity acceleration signals (tBodyAcc-XYZ and tGravityAcc-XYZ) using another low pass Butterworth filter with a corner frequency of 0.3 Hz.

561 features			1	2	3	4	5	6	7	8	9	10	11	12	13	14	15	16	17	18	19
Nº	Group	Measurement List	mean(): Mean value	std(): Standard deviation	mad(): Median absolute deviation	max(): Largest value in array	min(): Smallest value in array	sma(): Signal magnitude area	energy(): Energy measure. Sum of the squares divided by the number of values.	iqr(): Interquartile range	entropy(): Signal entropy	arCoeff(): Autorregresion coefficients with Burg order 1	arCoeff(): Autorregresion coefficients with Burg order 2	arCoeff(): Autorregresion coefficients with Burg order 3	arCoeff(): Autorregresion coefficients with Burg order 4	correlation(): correlation coefficient between two signals	maxInds(): index of the frequency component with largest magnitude	meanFreq(): Weighted average of the frequency components to obtain a mean frequency	skewness(): skewness of the frequency domain signal	kurtosis(): kurtosis of the frequency domain signal	bandsEnergy(): Energy of a frequency interval within the 64 bins of the FFT of each window.
1	Accelerometer	tBodyAcc-XYX	3	3	3	3	3	1	3	3	3	3	3	3	3	3					
2		tGravityAcc-XYZ	3	3	3	3	3	1	3	3	3	3	3	3	3	3					
3		tBodyAccJerk-XYZ	3	3	3	3	3	1	3	3	3	3	3	3	3	3					
4	Gyroscope	tBodyGyro-XYZ	3	3	3	3	3	1	3	3	3	3	3	3	3	3					
5		tBodyGyroJerk-XYZ	3	3	3	3	3	1	3	3	3	3	3	3	3	3					
6	magnitude Euclidean norm	tBodyAccMag	1	1	1	1	1	1	1	1	1	1	1	1	1						
7		tGravityAccMag	1	1	1	1	1	1	1	1	1	1	1	1	1						
8		tBodyAccJerkMag	1	1	1	1	1	1	1	1	1	1	1	1	1						
9		tBodyGyroMag	1	1	1	1	1	1	1	1	1	1	1	1	1						
10		tBodyGyroJerkMag	1	1	1	1	1	1	1	1	1	1	1	1	1						
11	FFT FOURIER	fBodyAcc-XYZ	3	3	3	3	3	1	3	3	3						3	3	3	3	42
12		fBodyAccJerk-XYX	3	3	3	3	3	1	3	3	3						3	3	3	3	42
13		fBodyGyro-XYX	3	3	3	3	3	1	3	3	3						3	3	3	3	42
14		fBodyAccMag	1	1	1	1	1	1	1	1	1						1	1	1	1	
15		fBodyAccJerkMag	1	1	1	1	1	1	1	1	1						1	1	1	1	
16		fBodyGyroMag	1	1	1	1	1	1	1	1	1						1	1	1	1	
17		fBodyGyroJerkMag	1	1	1	1	1	1	1	1	1						1	1	1	1	
18	Angle	angle(tBodyAccMean,gravity)	1																		
19		angle(tBodyAccJerkMean),gravityMean)	1																		
20		angle(tBodyGyroMean,gravityMean)	1																		
21		angle(tBodyGyroJerkMean,gravityMean)	1																		
22		angle(X,gravityMean)	1																		
23		angle(Y,gravityMean)	1																		
24		angle(Z,gravityMean)	1																		

Subsequently, the body linear acceleration and angular velocity were derived in time to obtain Jerk signals (tBodyAccJerk-XYZ and tBodyGyroJerk-XYZ). Also the magnitude of these three-dimensional signals were calculated using the Euclidean norm (tBodyAccMag, tGravityAccMag, tBodyAccJerkMag, tBodyGyroMag, tBodyGyroJerkMag).

561 features			1	2	3	4	5
Nº	Group	Measurement List	mean(): Mean value	std(): Standard deviation	mad(): Median absolute deviation	max(): Largest value in array	min(): Smallest value in array
1	**Accelerometer**	tBodyAcc-XYX	3	3	3	3	3
2		tGravityAcc-XYZ	3	3	3	3	3
3		tBodyAccJerk-XYZ	3	3	3	3	3
4	**Gyroscope**	tBodyGyro-XYZ	3	3	3	3	3
5		tBodyGyroJerk-XYZ	3	3	3	3	3
6		tBodyAccMag	1	1	1	1	1
7		tGravityAccMag	1	1	1	1	1

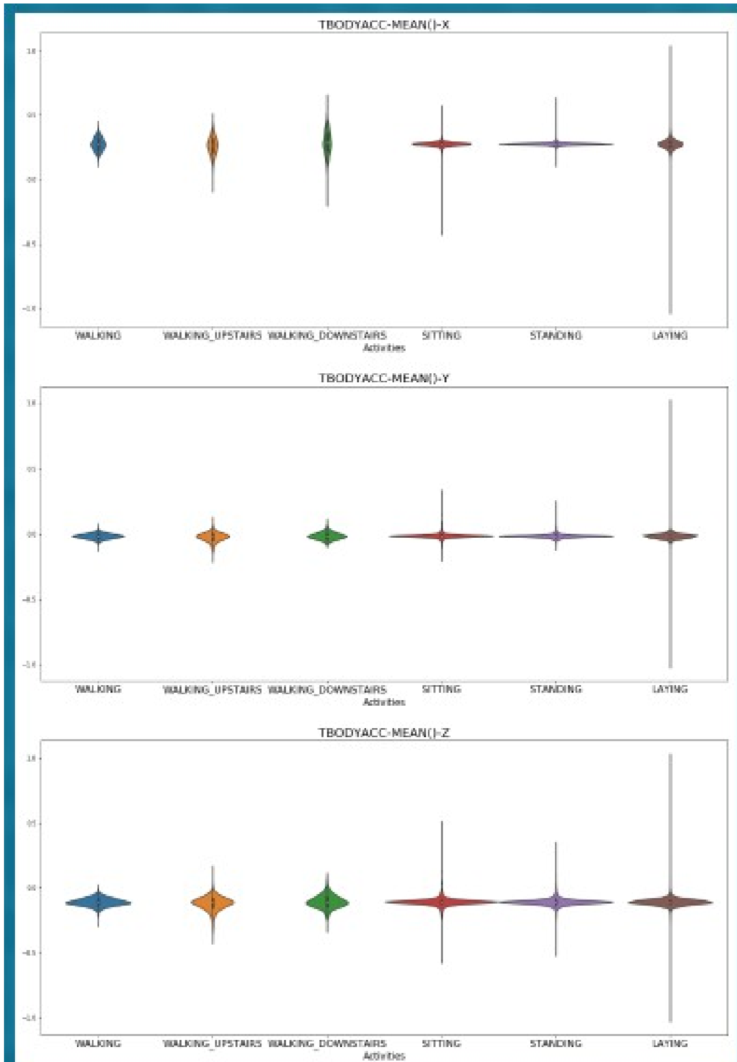

Accelerometer Body

<= Mean (X,Y,Z)

STD (X,Y,Z) =>

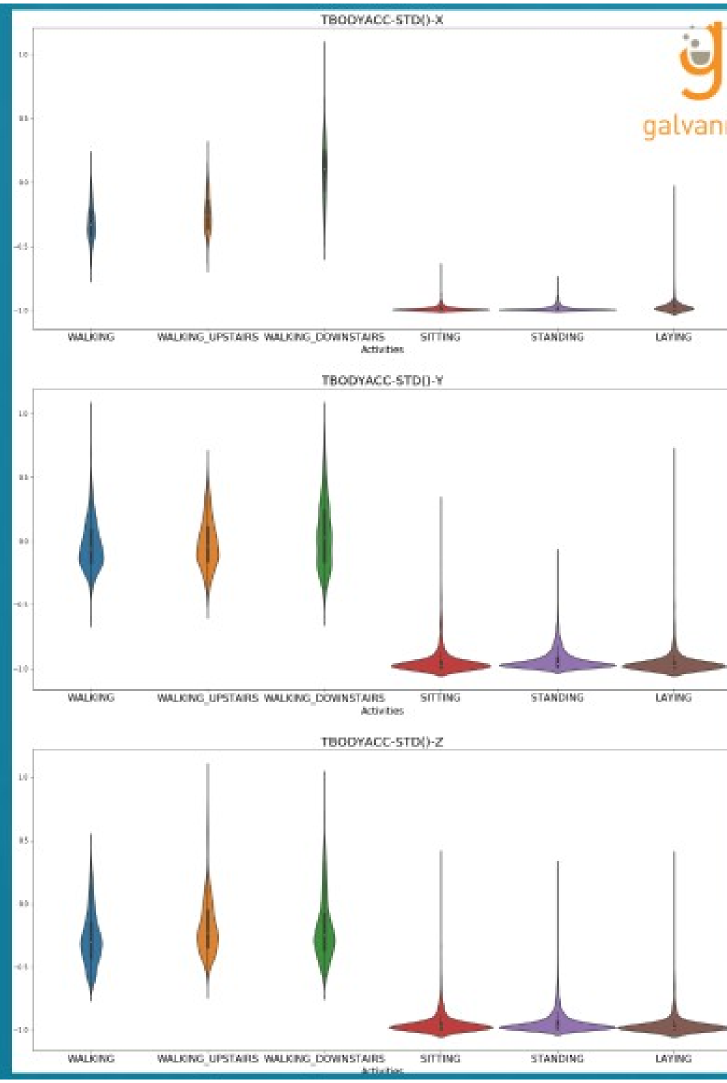

galvanize

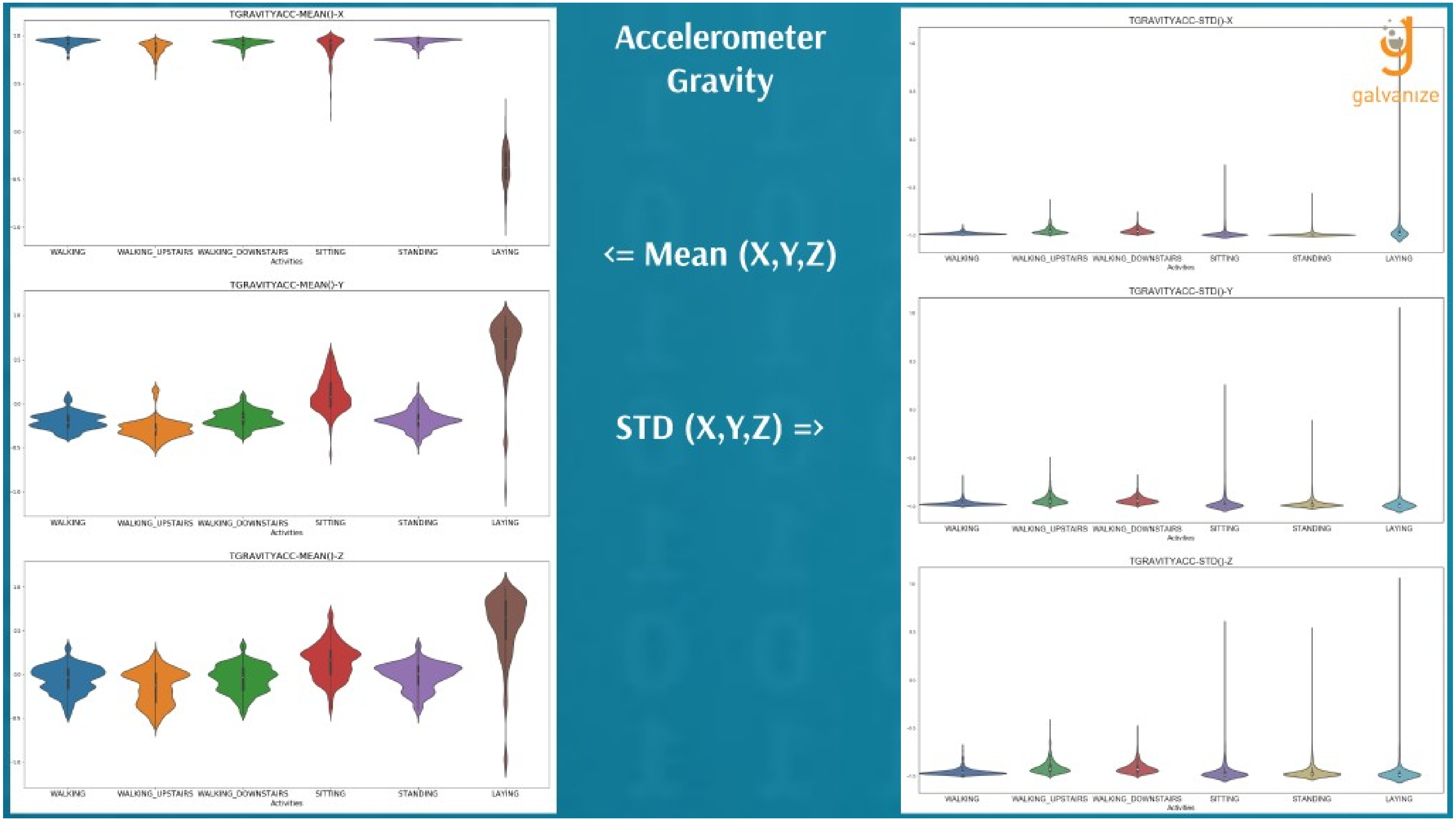

TGRAVITYACC-MEAN()-X
WALKING WALKING_UPSTAIRS WALKING_DOWNSTAIRS SITTING STANDING LAYING
Activities
TGRAVITYACC-MEAN()-Y
WALKING WALKING_UPSTAIRS WALKING_DOWNSTAIRS SITTING STANDING LAYING
Activities
TGRAVITYACC-MEAN()-Z
WALKING WALKING_UPSTAIRS WALKING_DOWNSTAIRS SITTING STANDING LAYING
Activities
Accelerometer Gravity
<= Mean (X,Y,Z)
STD (X,Y,Z) =>
TGRAVITYACC-STD()-X
galvanize
WALKING WALKING_UPSTAIRS WALKING_DOWNSTAIRS SITTING STANDING LAYING
Activities
TGRAVITYACC-STD()-Y
WALKING WALKING_UPSTAIRS WALKING_DOWNSTAIRS SITTING STANDING LAYING
Activities
TGRAVITYACC-STD()-Z
WALKING WALKING_UPSTAIRS WALKING_DOWNSTAIRS SITTING STANDING LAYING
Activities

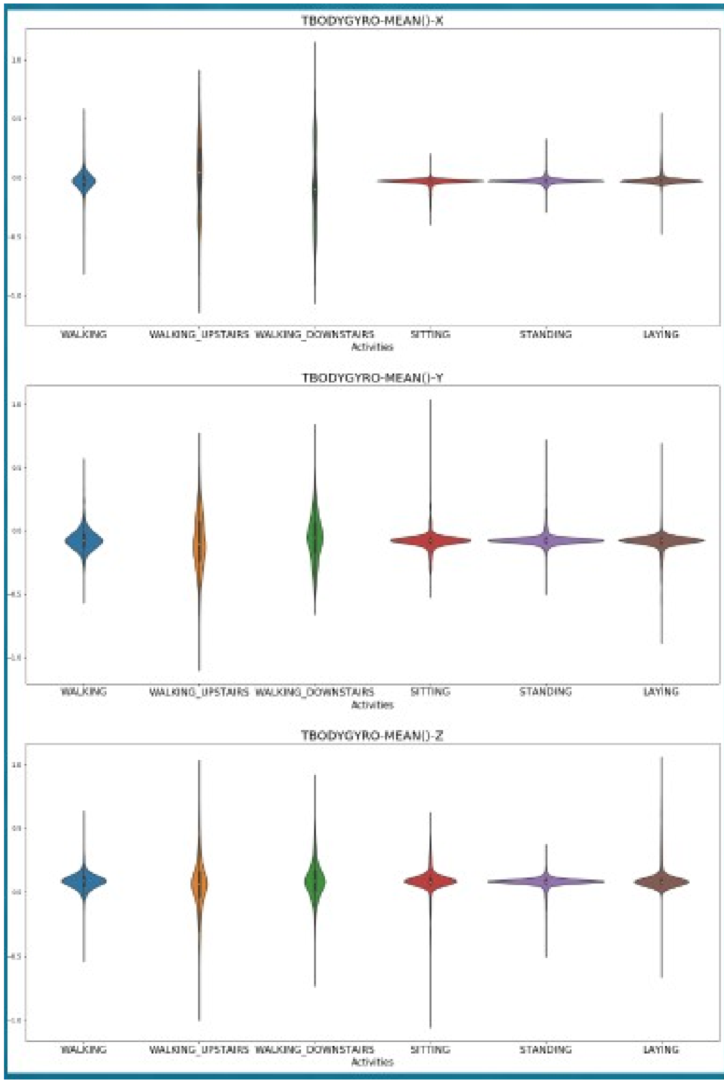

Gyroscope Body

<= Mean (X,Y,Z)

STD (X,Y,Z) =>

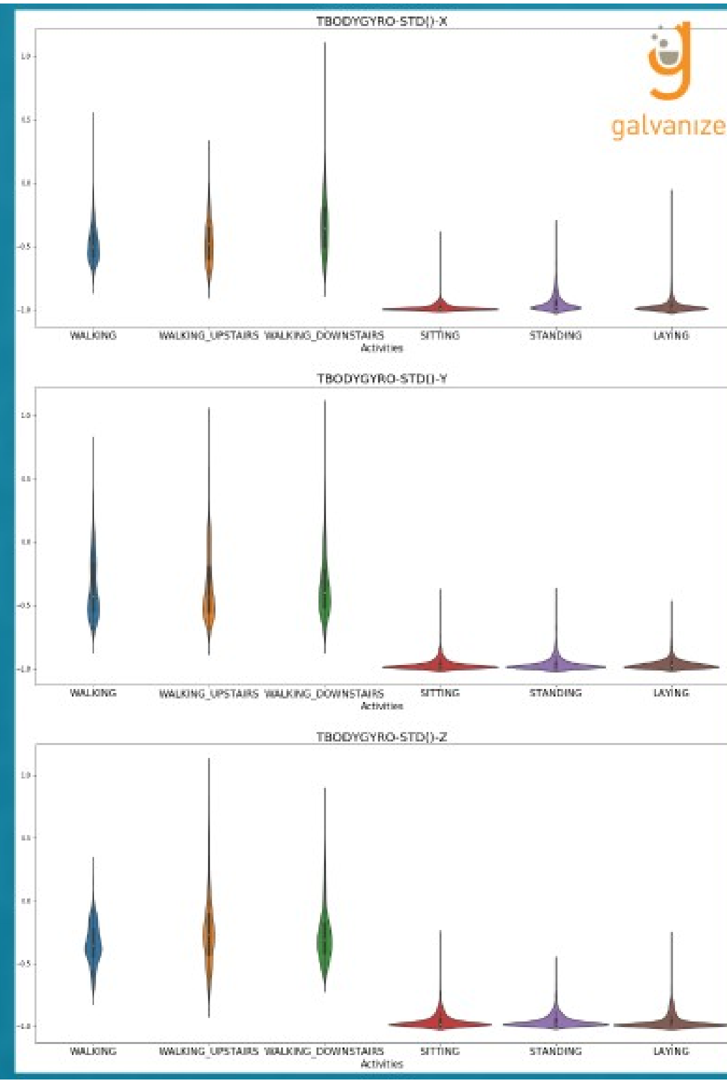

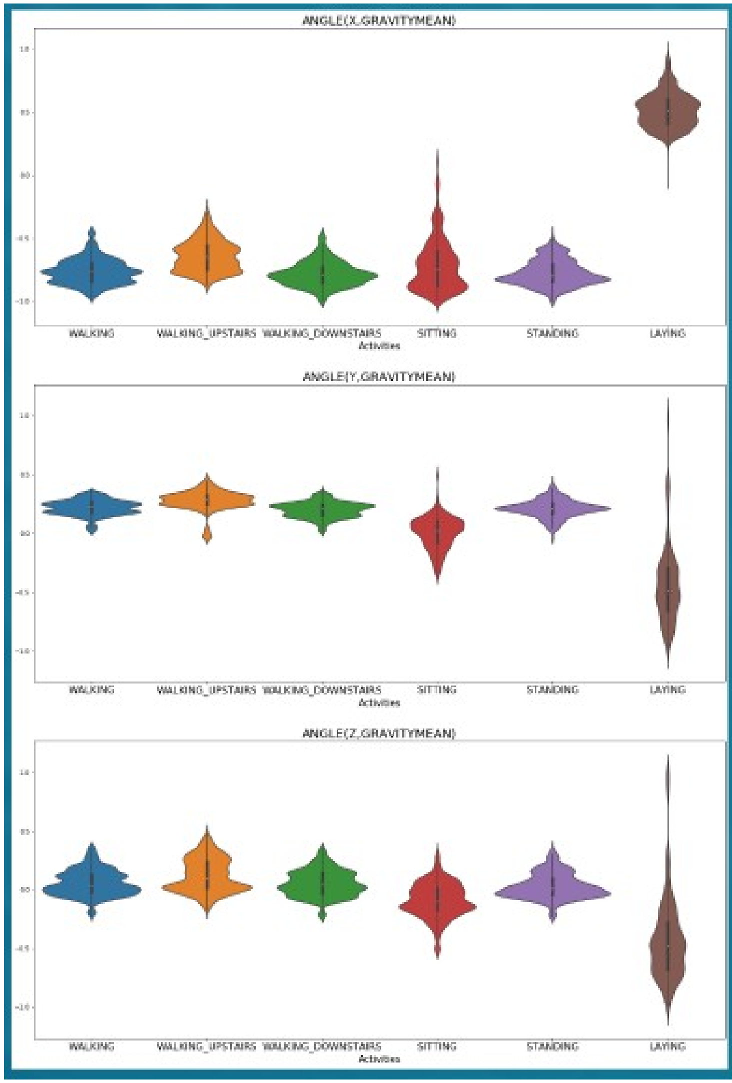

Angle Gravity

<= Mean (X,Y,Z)

galvanize

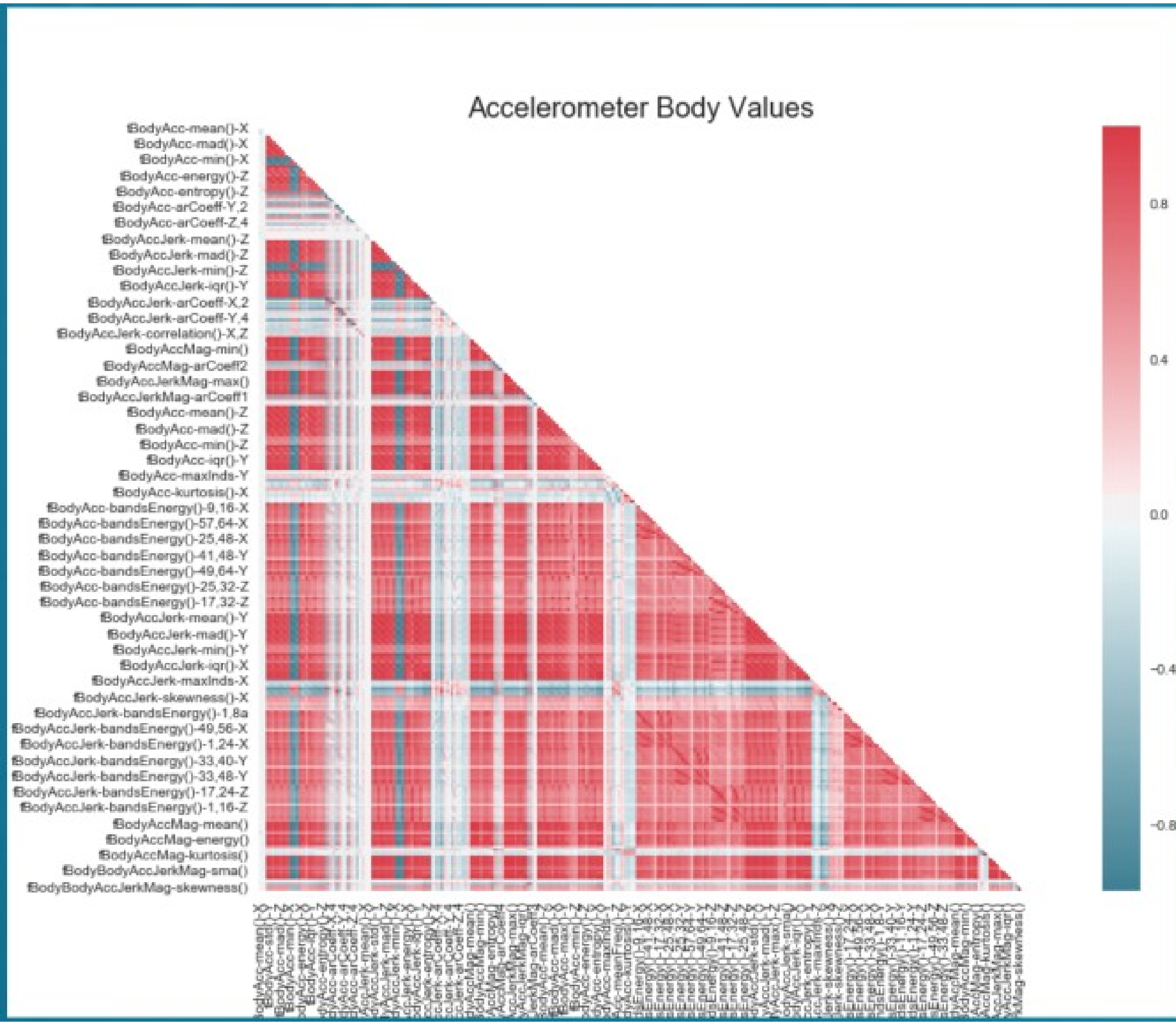
Accelerometer Body Values
fBodyAcc-mean()-X
fBodyAcc-mad()-X
fBodyAcc-min()-X
fBodyAcc-energy()-Z
fBodyAcc-entropy()-Z
fBodyAcc-arCoeff-Y,2
fBodyAcc-arCoeff-Z,4
fBodyAccJerk-mean()-Z
fBodyAccJerk-mad()-Z
fBodyAccJerk-min()-Z
fBodyAccJerk-iqr()-Y
fBodyAccJerk-arCoeff-X,2
fBodyAccJerk-arCoeff-Y,4
fBodyAccJerk-correlation()-X,Z
fBodyAccMag-min()
fBodyAccMag-arCoeff2
fBodyAccJerkMag-max()
fBodyAccJerkMag-arCoeff1
fBodyAcc-mean()-Z
fBodyAcc-mad()-Z
fBodyAcc-min()-Z
fBodyAcc-iqr()-Y
fBodyAcc-maxInds-Y
fBodyAcc-kurtosis()-X
fBodyAcc-bandsEnergy()-9,16-X
fBodyAcc-bandsEnergy()-57,64-X
fBodyAcc-bandsEnergy()-25,48-X
fBodyAcc-bandsEnergy()-41,48-Y
fBodyAcc-bandsEnergy()-49,64-Y
fBodyAcc-bandsEnergy()-25,32-Z
fBodyAcc-bandsEnergy()-17,32-Z
fBodyAccJerk-mean()-Y
fBodyAccJerk-mad()-Y
fBodyAccJerk-min()-Y
fBodyAccJerk-iqr()-X
fBodyAccJerk-maxInds-X
fBodyAccJerk-skewness()-X
fBodyAccJerk-bandsEnergy()-1,8a
fBodyAccJerk-bandsEnergy()-49,56-X
fBodyAccJerk-bandsEnergy()-1,24-X
fBodyAccJerk-bandsEnergy()-33,40-Y
fBodyAccJerk-bandsEnergy()-33,48-Y
fBodyAccJerk-bandsEnergy()-17,24-Z
fBodyAccJerk-bandsEnergy()-1,16-Z
fBodyAccMag-mean()
fBodyAccMag-energy()
fBodyAccMag-kurtosis()
fBodyBodyAccJerkMag-sma()
fBodyBodyAccJerkMag-skewness()
0.8
0.4
0.0
−0.4
−0.8

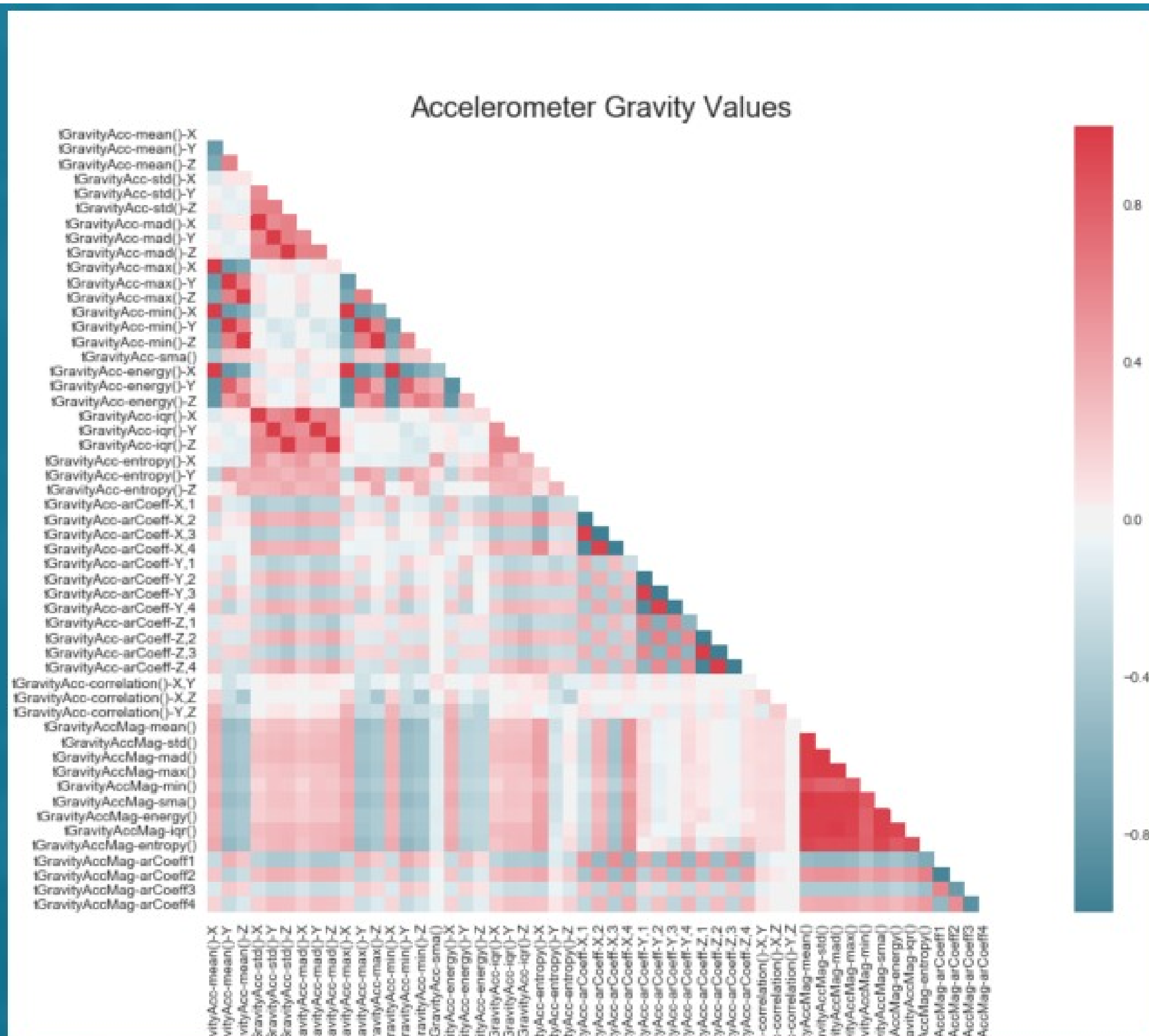
Accelerometer Gravity Values
tGravityAcc-mean()-X
tGravityAcc-mean()-Y
tGravityAcc-mean()-Z
tGravityAcc-std()-X
tGravityAcc-std()-Y
tGravityAcc-std()-Z
tGravityAcc-mad()-X
tGravityAcc-mad()-Y
tGravityAcc-mad()-Z
tGravityAcc-max()-X
tGravityAcc-max()-Y
tGravityAcc-max()-Z
tGravityAcc-min()-X
tGravityAcc-min()-Y
tGravityAcc-min()-Z
tGravityAcc-sma()
tGravityAcc-energy()-X
tGravityAcc-energy()-Y
tGravityAcc-energy()-Z
tGravityAcc-iqr()-X
tGravityAcc-iqr()-Y
tGravityAcc-iqr()-Z
tGravityAcc-entropy()-X
tGravityAcc-entropy()-Y
tGravityAcc-entropy()-Z
tGravityAcc-arCoeff-X,1
tGravityAcc-arCoeff-X,2
tGravityAcc-arCoeff-X,3
tGravityAcc-arCoeff-X,4
tGravityAcc-arCoeff-Y,1
tGravityAcc-arCoeff-Y,2
tGravityAcc-arCoeff-Y,3
tGravityAcc-arCoeff-Y,4
tGravityAcc-arCoeff-Z,1
tGravityAcc-arCoeff-Z,2
tGravityAcc-arCoeff-Z,3
tGravityAcc-arCoeff-Z,4
tGravityAcc-correlation()-X,Y
tGravityAcc-correlation()-X,Z
tGravityAcc-correlation()-Y,Z
tGravityAccMag-mean()
tGravityAccMag-std()
tGravityAccMag-mad()
tGravityAccMag-max()
tGravityAccMag-min()
tGravityAccMag-sma()
tGravityAccMag-energy()
tGravityAccMag-iqr()
tGravityAccMag-entropy()
tGravityAccMag-arCoeff1
tGravityAccMag-arCoeff2
tGravityAccMag-arCoeff3
tGravityAccMag-arCoeff4
0.8
0.4
0.0
-0.4
-0.8

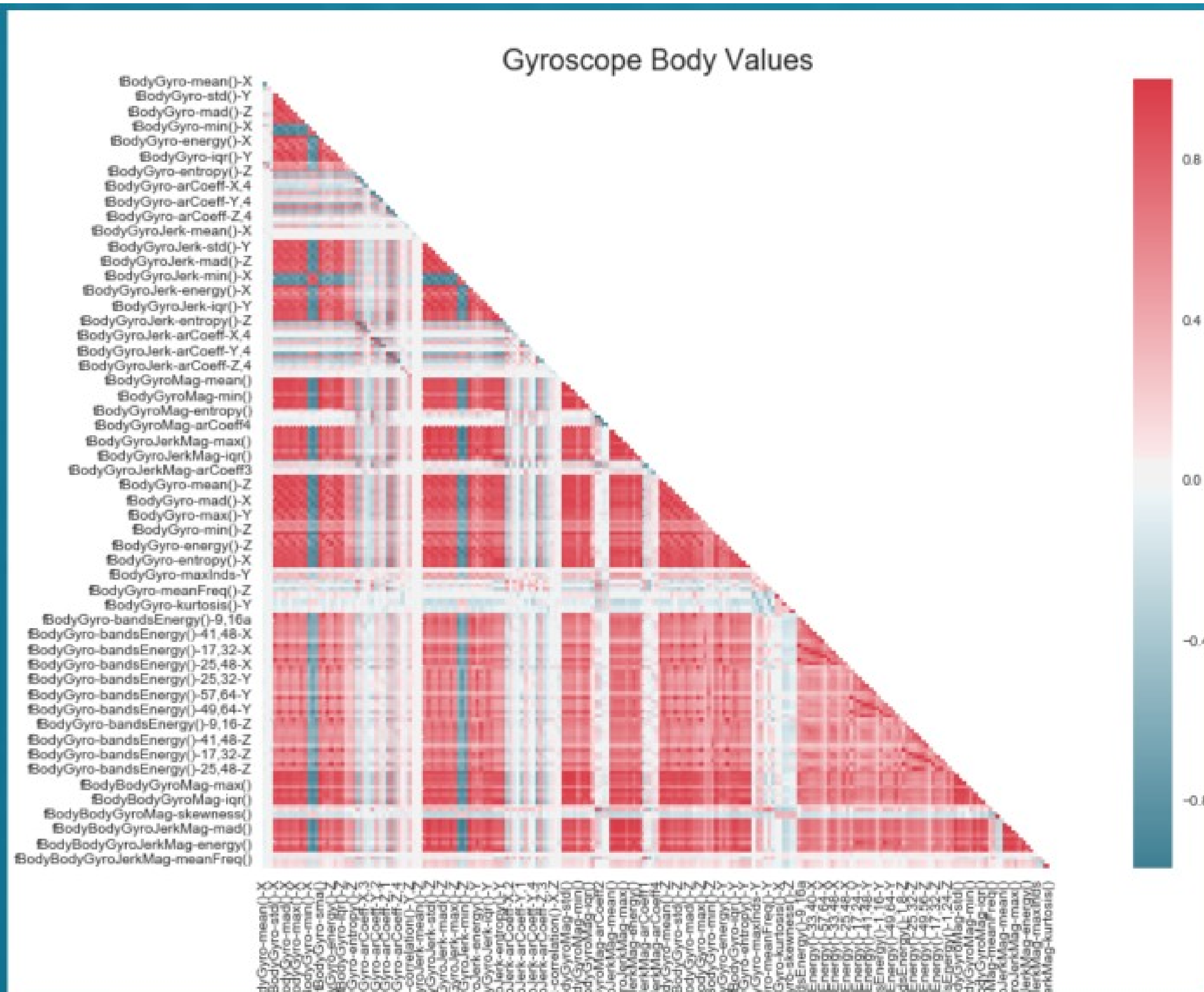
Gyroscope Body Values
fBodyGyro-mean()-X
fBodyGyro-std()-Y
fBodyGyro-mad()-Z
fBodyGyro-min()-X
fBodyGyro-energy()-X
fBodyGyro-iqr()-Y
fBodyGyro-entropy()-Z
fBodyGyro-arCoeff-X,4
fBodyGyro-arCoeff-Y,4
fBodyGyro-arCoeff-Z,4
fBodyGyroJerk-mean()-X
fBodyGyroJerk-std()-Y
fBodyGyroJerk-mad()-Z
fBodyGyroJerk-min()-X
fBodyGyroJerk-energy()-X
fBodyGyroJerk-iqr()-Y
fBodyGyroJerk-entropy()-Z
fBodyGyroJerk-arCoeff-X,4
fBodyGyroJerk-arCoeff-Y,4
fBodyGyroJerk-arCoeff-Z,4
fBodyGyroMag-mean()
fBodyGyroMag-min()
fBodyGyroMag-entropy()
fBodyGyroMag-arCoeff4
fBodyGyroJerkMag-max()
fBodyGyroJerkMag-iqr()
fBodyGyroJerkMag-arCoeff3
fBodyGyro-mean()-Z
fBodyGyro-mad()-X
fBodyGyro-max()-Y
fBodyGyro-min()-Z
fBodyGyro-energy()-Z
fBodyGyro-entropy()-X
fBodyGyro-maxInds-Y
fBodyGyro-meanFreq()-Z
fBodyGyro-kurtosis()-Y
fBodyGyro-bandsEnergy()-9,16a
fBodyGyro-bandsEnergy()-41,48-X
fBodyGyro-bandsEnergy()-17,32-X
fBodyGyro-bandsEnergy()-25,48-X
fBodyGyro-bandsEnergy()-25,32-Y
fBodyGyro-bandsEnergy()-57,64-Y
fBodyGyro-bandsEnergy()-49,64-Y
fBodyGyro-bandsEnergy()-9,16-Z
fBodyGyro-bandsEnergy()-41,48-Z
fBodyGyro-bandsEnergy()-17,32-Z
fBodyGyro-bandsEnergy()-25,48-Z
fBodyBodyGyroMag-max()
fBodyBodyGyroMag-iqr()
fBodyBodyGyroMag-skewness()
fBodyBodyGyroJerkMag-mad()
fBodyBodyGyroJerkMag-energy()
fBodyBodyGyroJerkMag-meanFreq()
0.8
0.4
0.0
-0.4
-0.8


2º Capstone Project
Human Activity Recognition
Using Smartphones
Train
& Test
Features
Dataset
galvanize
Nei Rosa da Costa
April - 2018

PCA (36 components)

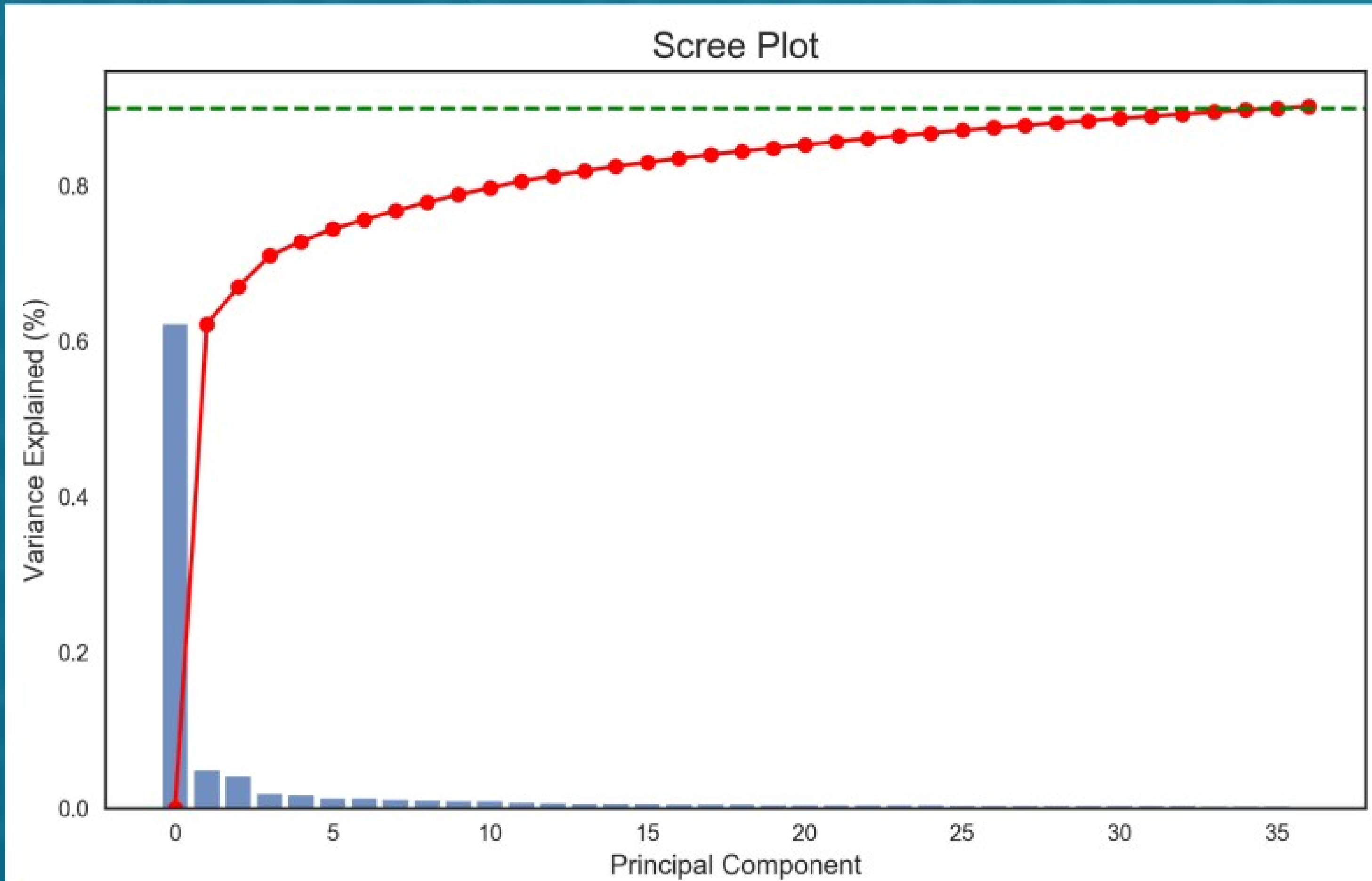

PCA variance ratio

Nº Component	%
1	62.23%
2	67.00%
3	71.02%
4	72.84%
5	74.45%
6	75.65%
7	76.84%
.	
.	
.	
.	
30	88.69%
31	88.97%
32	89.24%
33	89.51%
34	89.75%
35	89.99%
36	90.22%


2º Capstone Project
Human Activity Recognition
Using Smartphones
Train
& Test
Features
Dataset
galvanize
Nei Rosa da Costa
April - 2018

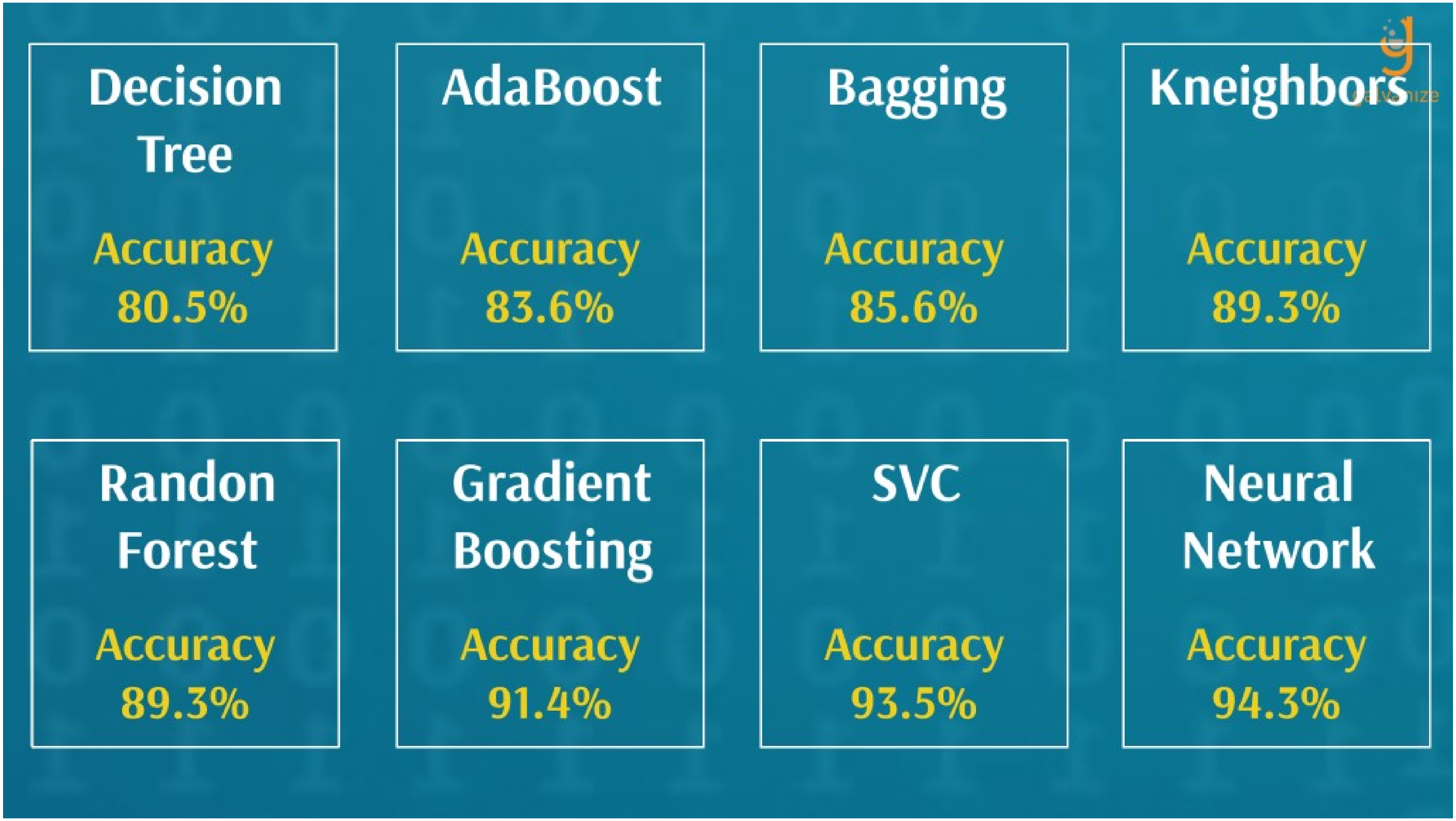
Decision Tree
Accuracy 80.5%
AdaBoost
Accuracy 83.6%
Bagging
Accuracy 85.6%
Kneighbors
Accuracy 89.3%
Randon Forest
Accuracy 89.3%
Gradient Boosting
Accuracy 91.4%
SVC
Accuracy 93.5%
Neural Network
Accuracy 94.3%

Decision Tree (Worst Accuracy)

REAL	PREDICT						PRECISION
	WALKING	WALKING UPSTAIRS	WALKING DOWNSTAIRS	SITTING	STANDING	LAYING	
WALKING	446	24	26				89,92%
WALKING UPSTAIRS	91	350	29			1	74,31%
WALKING DOWNSTAIRS	49	55	316				75,24%
SITTING		1		341	149		69,45%
STANDING				116	414	2	77,82%
LAYING				22	11	504	93,85%

Decision Tree
Accuracy
80.5%

AdaBoost
Accuracy
83.6%

Bagging
Accuracy
85.6%

Kneighbors
Accuracy
89.3%

Randon Forest
Accuracy
89.3%

Gradient Boosting
Accuracy
91.4%

SVC
Accuracy
93.5%

Neural Network
Accuracy
94.3%

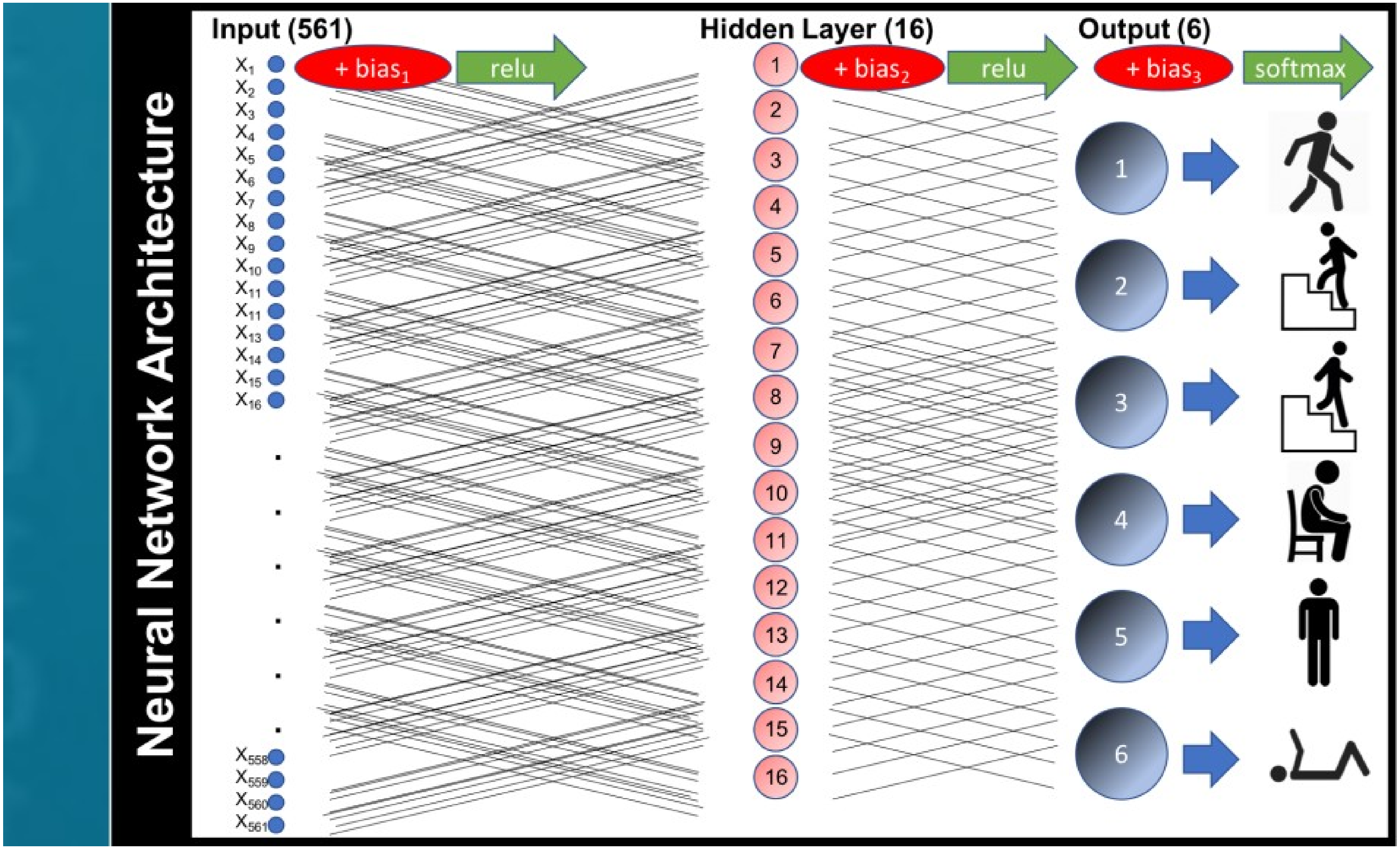

Neural Network Architecture
Input (561)
Hidden Layer (16)
Output (6)
+ bias$_1$
relu
+ bias$_2$
relu
+ bias$_3$
softmax
X_1
X_2
X_3
X_4
X_5
X_6
X_7
X_8
X_9
X_{10}
X_{11}
X_{11}
X_{13}
X_{14}
X_{15}
X_{16}
X_{558}
X_{559}
X_{560}
X_{561}
1
2
3
4
5
6
7
8
9
10
11
12
13
14
15
16
1
2
3
4
5
6

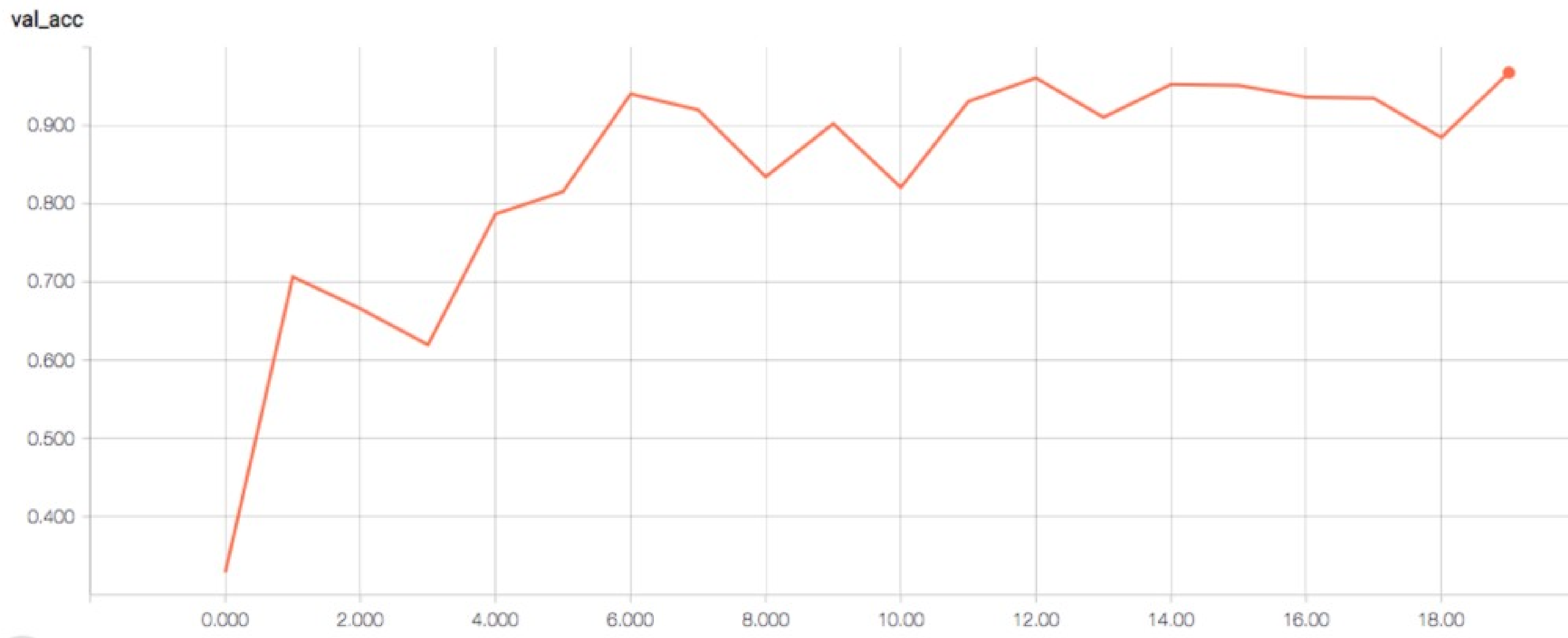
val_acc
0.900
0.800
0.700
0.600
0.500
0.400
0.000
2.000
4.000
6.000
8.000
10.00
12.00
14.00
16.00
18.00

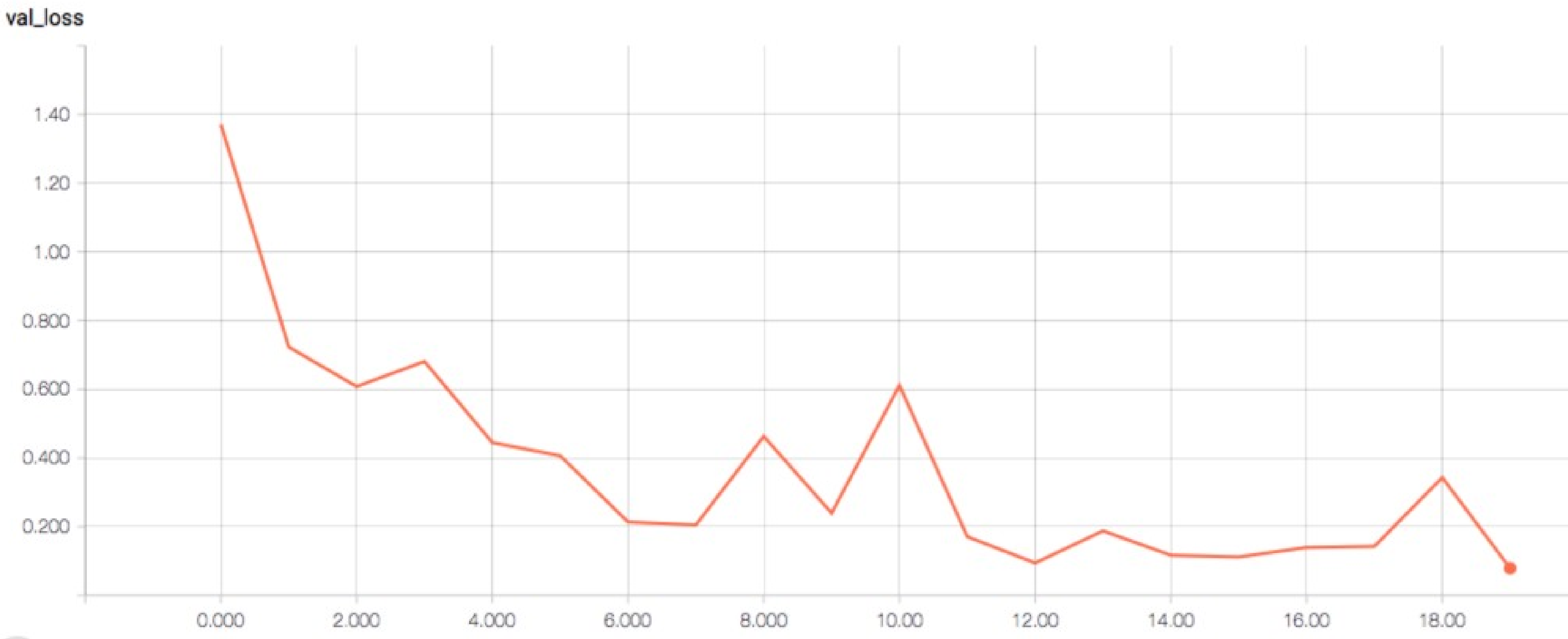
val_loss
1.40
1.20
1.00
0.800
0.600
0.400
0.200
0.000
2.000
4.000
6.000
8.000
10.00
12.00
14.00
16.00
18.00

Neural Network (Best Accuracy)

REAL	PREDICT						PRECISION
	WALKING	WALKING UPSTAIRS	WALKING DOWNSTAIRS	SITTING	STANDING	LAYING	
WALKING	486	5	5				97,98%
WALKING UPSTAIRS	21	435	10		5		92,36%
WALKING DOWNSTAIRS	4	13	403				95,95%
SITTING				477	13	1	97,15%
STANDING	1			75	456		85,71%
LAYING				16		521	97,02%

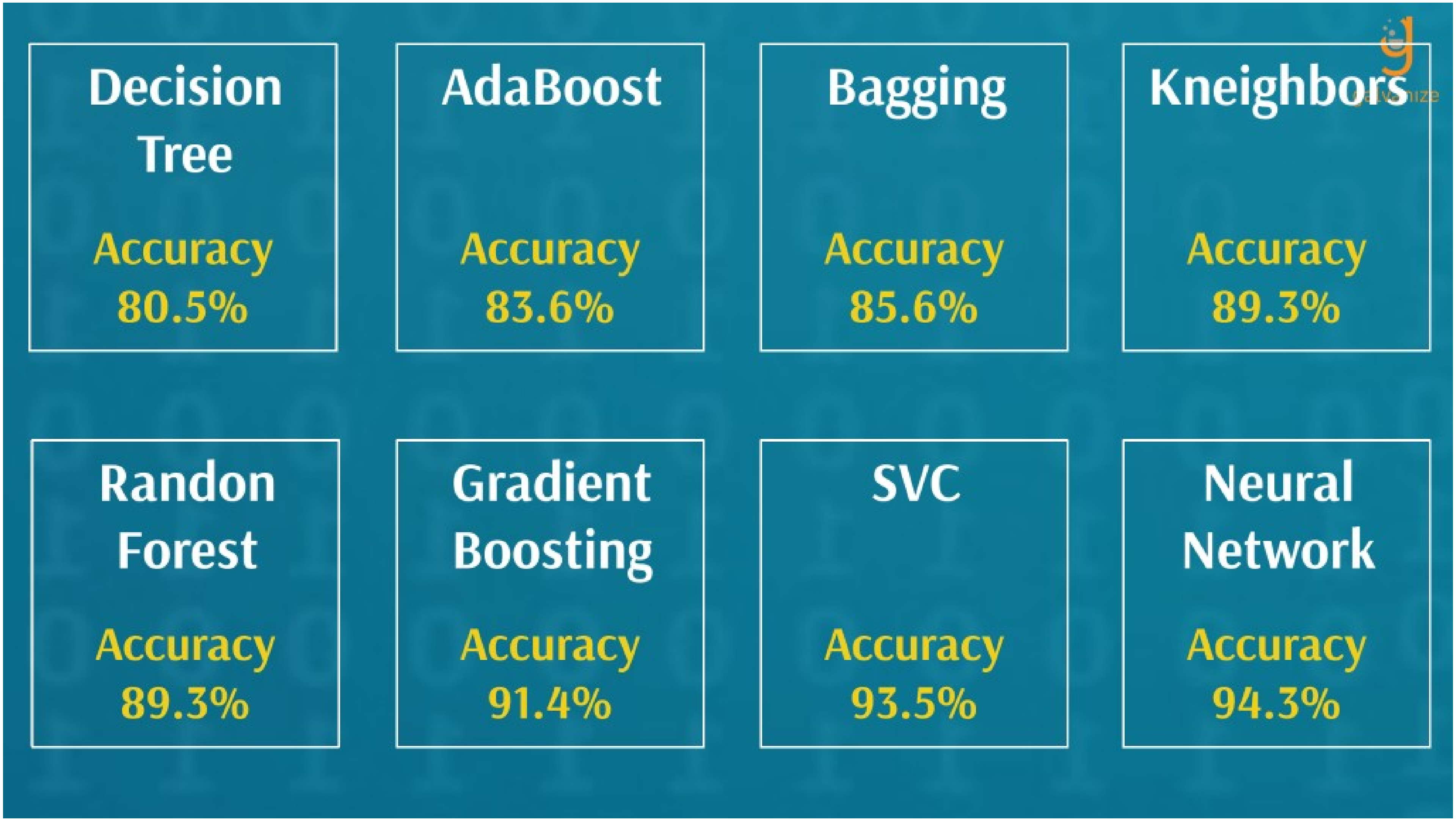
Decision Tree
Accuracy 80.5%
AdaBoost
Accuracy 83.6%
Bagging
Accuracy 85.6%
Kneighbors
Accuracy 89.3%
Randon Forest
Accuracy 89.3%
Gradient Boosting
Accuracy 91.4%
SVC
Accuracy 93.5%
Neural Network
Accuracy 94.3%


2º Capstone Project
Human Activity Recognition
Using Smartphones
Train
& Test
Features
Dataset
galvanize
Nei Rosa da Costa
April - 2018

Conclusion:

- The identification of activities through the analysis of the measurements generated by the cell phone is possible with a good precision;

- The neural network presented better results than other classification models

  OBS: The Support Vector Machine (SVM), working with all predictors (561), without using PCA, presented superior accuracy to neural network);

- The use of this methodology can allow the creation of applications that identify the type of activity developed by the user while carrying his cell phone next to the body.


Thanks!

galvanize

Conclusion:

- The identification of activities through the analysis of the measurements generated by the cell phone is possible with a good precision;

- The neural network presented better results than other classification models

  OBS: The Support Vector Machine (SVM), working with all predictors (561), without using PCA, presented superior accuracy to neural network);

- The use of this methodology can allow the creation of applications that identify the type of activity developed by the user while carrying his cell phone next to the body.


2º Capstone Project
Human Activity Recognition
Using Smartphones
Train
& Test
Features
Dataset
galvanize
Nei Rosa da Costa
April - 2018